



Deepening of lipidome annotation by associating cross-metathesis reaction with mass spectrometry: application to an in vitro model of corneal toxicity

Romain Magny^{1,2} · Anne Regazzetti² · Karima Kessal^{1,3} · Christophe Baudouin^{1,3,4,5} · Stéphane Mélik-Parsadaniantz¹ · Olivier Laprévotte^{2,6} · Françoise Brignole-Baudouin^{1,2,3} · Nicolas Auzeil² · Emmanuel Roulland²

Received: 13 April 2021 / Revised: 20 May 2021 / Accepted: 26 May 2021
© Springer-Verlag GmbH Germany, part of Springer Nature 2021

Abstract

The in-depth knowledge of lipid biological functions needs a comprehensive structural annotation including a method to locate fatty acid unsaturations, which remains a thorny problem. For this purpose, we have associated Grubbs' cross-metathesis reaction and liquid chromatography hyphenated to tandem mass spectrometry to locate double bond positions in lipid species. The pretreatment of lipid-containing samples by Grubbs' catalyst and an appropriate alkene generates substituted lipids through cross-metathesis reaction under mild, chemoselective, and reproducible conditions. A systematic LC-MS/MS analysis of the reaction mixture allows locating unambiguously the double bonds in fatty acid side chains of phospholipids, glycerolipids, and sphingolipids. This method has been successfully applied at a nanomole scale to commercial standard mixtures consisting of 10 lipid subclasses as well as in lipid extracts of human corneal epithelial (HCE) cell line allowing to pinpoint double bond of more than 90 species. This method has also been useful to investigate the lipid homeostasis alteration in an in vitro model of corneal toxicity, *i.e.*, HCE cells incubated with benzalkonium chloride. The association of cross-metathesis and tandem mass spectrometry appears suitable to locate double bond positions in lipids involved in relevant biological processes.

Keywords Double bond location · Cross-metathesis · Tandem mass spectrometry · Lipidomics · Corneal toxicity

Nicolas Auzeil and Emmanuel Roulland contributed equally to this work.

✉ Nicolas Auzeil
nicolas.auzeil@parisdescartes.fr

✉ Emmanuel Roulland
emmanuel.roulland@parisdescartes.fr

¹ Sorbonne Université, INSERM, CNRS, Institut de la Vision, 75012 Paris, France

² C-TAC, CiTCoM, UMR 8038, CNRS Université de Paris, Faculté de Pharmacie, 75006 Paris, France

³ CHNO des Quinze-Vingts, INSERM-DGOS CIC 1423, 75012 Paris, France

⁴ Département d'Ophthalmologie, Hôpital Ambroise Paré, AP HP, 92100 Boulogne, France

⁵ Université Versailles St Quentin en Yvelines, 78180 Paris Saclay, Montigny-Le-Bretonneux, France

⁶ Hôpital Européen Georges Pompidou, AP-HP, Service de Biochimie, 75015 Paris, France

Introduction

Lipids are an essential class of metabolites playing a pleiotropic role in cells depending on their structures, the latter being actually very variable [1, 2]. According to the international LipidMaps consortium, molecules arising from isoprene subunit condensation define the sterols or prenol lipid class, while lipids resulting from ketoacyl subunit condensation belong to the classes of fatty acids (FA), glycerolipids (GL), glycerophospholipids (PL), and sphingolipids (SL) [3, 4]. Within these latter classes, the structural diversity mainly originates from the nature of the fatty acid side chain, *i.e.*, the chain length and the number and location of unsaturations. The location of double bonds in the FA chain is of prime relevance as it may determine the biological activity of a given lipid [5, 6]. For example, ω -3 polyunsaturated FA (PUFA) display anti-inflammatory properties, while in contrast, ω -6 ones mainly act as pro-inflammatory metabolites. In ocular surface diseases, ω -3 PUFA has been shown to increase

corneal wound healing and nerve regeneration through docosanoid biosynthesis [7, 8]. Regarding mono-unsaturated fatty acid (MUFA) species, a shift from $\Delta 9$ to $\Delta 11$ C=C isomers in phosphatidylcholines (PC) and phosphatidylethanolamines (PE) containing octadecenoic acid (18:1) has been reported in the plasma of type 2 diabetic patients [9]. Consequently, to clarify the role of lipids in physiological processes, it is valuable to determine the double bond location in FA side chains of lipids.

For two decades, mass spectrometry (MS) has been increasingly used to study lipids [10]. Lipidomic analysis mainly uses liquid chromatography hyphenated to electrospray high-resolution tandem mass spectrometry (LC-MS/MS) [11]. Indeed, LC-MS/MS analysis is highly suitable to identify polar head groups, and therefore lipid subclasses but also FA chains [11, 12]. However, LC-MS/MS alone do not allow to identify position isomers when unsaturated FA are involved [13], unless using sophisticated analytical approaches implementing ion activation techniques, such as ultraviolet photodissociation (UVPD) or ozone-induced dissociation (OzID) [14, 15]. These methods also include online derivatization such as the Paterno-Buchi (PB) photochemical reaction prior to MS analysis [9, 16, 17]. Nevertheless, these online methods involving sample derivatization require technical adaptations of the mass spectrometer to be routinely used: UVPD, an hybrid MS^3 CID/UV mass spectrometer; OzID, the introduction of ozone within the collision cell; and PB, the use of an UV lamp inside or proximal to the ion source. Regarding offline sample preparation, a derivatization step based on an epoxidation reaction has been proposed to identify double bond lipid isomers [18]. Albeit very suitable for MUFA species, this approach did not allow identifying double bond isomers in PUFA species readily.

Cross-metathesis (CM) is a highly chemoselective, functional group-tolerant reaction carried out under mild conditions, so it appeared particularly suitable for lipid isomer analysis. Indeed, biologically occurring MUFA and PUFA species contain one or several but-2-en-1,4-ylidene moieties, these alkenes belong with category II in the Grubbs' CM classification [19]. Accordingly, they should react readily with appropriate alkenes using Ru carbene complexes such as the commercially available second-generation Grubbs' catalyst easily giving CM product. It can be anticipated that based on the LC-MS data analysis of the CM products, the location of lipid double bonds would be easily and unequivocally determined (Scheme 1). In a previous study, double bond location was determined in FA species using CM and mass spectrometry [20]. However, the CM conditions used in this study are classical and well adapted to pure and structurally simple FAs at the milligram scale; however, it is not operationally adaptable to small biological samples consisting in a mixture of hundreds of complex lipids belonging to all classes. In this case, FAs are mainly esterified within phospholipids, sphingolipids,

or glycerolipids which altogether form a huge structural diversity we wish to explore using CM. The aim of the present study was thus to associate CM and MS to define a reproducible and routinely usable protocol allowing an identification of lipid isomers. The proposed method was applied to biological samples, *i.e.*, human corneal epithelial cell line used as a toxicological model of dry eye disease.

Materials and methods

Chemicals and reagents

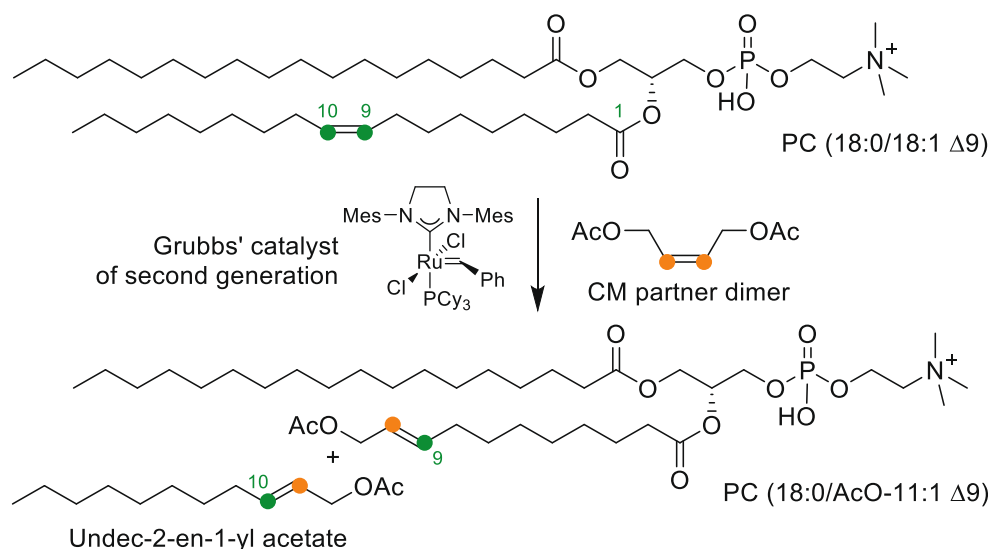
Chloroform (Carlo Erba Reactifs SDS, Val-de-Reuil, France), acetonitrile, methanol, isopropanol, water of LC-MS grade (J.T. Baker, Phillipsburg, NJ, USA), and 3,5-di-tert-4-butylhydroxytoluene (Sigma Aldrich, Saint-Quentin Fallavier, France) were used to perform cell lipid extraction and to prepare mobile phase for liquid chromatography. All commercial lipid standards were purchased from Avanti Polar Lipids, Inc. (Alabaster, AL, USA) and are listed in Table S1 of the Supplementary Information (ESM). Grubbs' catalyst of second generation (CAS Number: 246047-72-3) was purchased at MERCK and was used as received with no further purification. All cross-metathesis reactions were performed using anhydrous dichloromethane as solvent under an argon atmosphere. Dichloromethane (CH_2Cl_2) is obtained through distillation over calcium hydride (CaH_2) under argon. All the reagent grade chemicals obtained from commercial sources were used as received.

Sample preparation of lipids

Preparation of lipid standards A volume of 200 μ L of a 1-mM stock solution containing the commercial lipid standards (2 nmol) was added to a tube and was then evaporated under reduced pressure at 45 °C.

Lipid extraction of HCE cells Human corneal epithelial (HCE) cell line used in this study was purchased from the RIKEN biobank (Tsukuba, Japan) [21]. Lipid extraction of HCE cells was done as previously described [22]. Briefly, both benzalkonium chloride (BAK) incubated- and control-HCE cells were harvested using trypsin-EDTA 0.05%, washed with DPBS, centrifuged at 2000 rpm for 10 min. Dry cell pellets were adjusted to 3 million cells and stored at -80°C until analysis. After thawing, the cell pellets were resuspended in ultrapure water (1 mL) and were sonicated for 5 min. Lipids were extracted using a chloroform/methanol/water (5:5:2, v/v/v) mixture containing 3,5-di-tert-4-butylhydroxytoluene 0.01% (w/v) as antioxidant agent. Samples were subsequently centrifuged at 3000 rpm for 10 min, organic phases were collected, and solvents were evaporated under reduced pressure at 45 °C.

Scheme 1 Cross-metathesis reaction applied to PC (18:0/18:1 Δ^9)



HCl pretreatment Prior to cross-metathesis reaction, the dry commercial lipid standards and the cell lipid extracts were pre-treated with 1 M HCl to prevent the deleterious effect of basic amine on Grubbs' catalysts.

Method for the cross-metathesis reaction

The general procedure for cross-metathesis performed on small-scale samples of lipids was as follows.

Catalyst pre-activation A Schlenk tube charged with Grubbs' catalyst of second generation (12.2 mg, 0.014 mmol) was flushed with argon; then, CH_2Cl_2 (2 mL) and (Z)-but-2-ene-1,4-diyl diacetate (114 μL , 0.715 mmol) were introduced. The tube was sealed and stirred at 40 °C for 2 h.

Cross-metathesis on lipid samples The 1/100 or 1/1000 diluted solutions were prepared by introducing respectively 100 μL or 10 μL of the above reaction mixture in a round-bottom flask containing dry CH_2Cl_2 (10 mL) under argon. To vials containing *circa* 20 nmol or 2 nmol of lipids where 300 μL of the 1/100 solution or 1/1000 respectively was added, the solvent was then removed with a flux of argon. Once evaporated, the vials were sealed and heated at the desired temperature for the desired period of time. The content of each vial was then diluted in 100 μL of a $\text{CHCl}_3/\text{MeCN}/\text{H}_2\text{O}/i\text{-PrOH}$ (20/30/10/30, v/v) mixture and 5 μL was injected in the LC-MS/MS system as described hereafter and according to our previous published methods [22–24].

Data-dependent LC-ESI-HRMS/MS analysis

The analysis of lipid extracts by liquid chromatography using positive and negative electrospray ionization mass spectrometry was achieved on a UPLC[®] system (Waters, Manchester,

UK) hyphenated to a Synapt[®] G2 (Q-TOF) mass spectrometer (Waters) [25]. The chromatographic separation was performed on an Acquity[®] CSH C18 column (100 mm \times 2.1 mm; 1.7 μm). A binary gradient system was used for the elution and consists in 10 mM ammonium acetate in acetonitrile/water mixture (40:60, v/v) as solvent A and 10 mM ammonium acetate in acetonitrile/isopropanol mixture (10:90, v/v) as solvent B. Eluent increased from 40% B to 100% B in 10 min and was held at 100% B for 2 min before returning to 40% B. The flow rate was kept at 0.4 mL min⁻¹, the column oven was set at 50°C, and the injection volume was 5 μL . The source parameters were as follows: capillary voltage 3000 V (ESI+) and 2400 V (ESI-), cone voltage 30 V (ESI+) and 45 V (ESI-), source temperature 120°C, desolvation temperature 550°C, cone gas flow 20 L/h, and desolvation gas flow 1000 L/h. Leucine enkephalin (2 ng mL⁻¹) was used as an external reference compound (Lock-Spray[™]) for mass correction. In data-dependent acquisition mode (DDA), a full MS scan was first acquired and then followed by 5 MS/MS scans performed on the most intense ions above an absolute threshold of 1000 counts. Precursor ions were selected by the quadrupole with a window size of 1.0 Th and fragmented at collision energy ramping from 20 to 40 eV. The duration of MS and MS/MS scans was 0.2 s. Data were acquired between m/z 50 and 1200 using a resolution of 20,000 FWHM at m/z 500 in the full scan mode. Data acquisition was managed using Waters MassLynx[™] software (version 4.1; Waters MS Technologies).

Data preprocessing parameters

For positive and negative ion modes, raw data files were converted into open-source mzXML file with MSConvert 3.0 and the data processing was then performed using MZmine 2.5 software as previously described [22]. Briefly, MS and MS/

MS spectra were extracted with a mass detection noise level set at 1E2 and 0E0, respectively. The ADAP algorithm was used to build chromatograms (minimum group size of 5 scans, a group intensity threshold of 1000, and an m/z tolerance of 10 ppm) [26]. The settings for ADAP wavelet chromatogram deconvolution algorithm were as follows: signal to noise ratio = 10, coefficient/area ratio = 60, peak duration range = 0.05–0.5 min, retention time wavelet range = 0.0–0.2. The isotopic peak grouper algorithm was then used to de-isotope chromatograms using a m/z and a retention time (t_R) tolerance of respectively 10 ppm and 0.1 min. Peak alignment was achieved with join aligner method using parameters as follows: m/z and t_R tolerance of respectively 10 ppm and 0.15 min. MS/MS scans were then associated with their corresponding MS scans using a m/z and t_R tolerance of respectively 10 ppm and 0.15 min. Gap filling process was then performed on the peak list using the so-called module “same RT and m/z range gap filler” with m/z tolerance of 10 ppm. Lipids were then annotated based on exact mass measurement and retention time with the “custom database” module using an in-house database. These data preprocessing steps led to two distinct matrixes, both in ESI+ and ESI– mode, listing for annotated lipid m/z , t_R , and peak area values. These matrixes were normalized and filtered as previously described [23].

Identification of lipids

The structure assignment of lipid species was based on MS and MS/MS data, using a tolerance window of 5 and 15 ppm, respectively. Identification was supported by t_R values through comparison of experimental to expected values calculated using t_R prediction models. Indeed, in reverse-phase liquid chromatography, there is a linear relationship between retention time and equivalent carbon number (ECN) as previously described [22, 23]. MS/MS data was used to fully determine phospholipid fatty acid composition. Fatty acyl sn_1 and sn_2 position was determined in negative ion mode using the relative intensity of ions corresponding to carboxylates as previously described [22, 27].

Following the identification of lipids at the fatty acid side chain level, cross-metathesis products was analyzed to identify the double bond position within fatty acid side chains. The structure assignment of CM products was also based on MS and MS/MS data using a tolerance window of 5 and 15 ppm, respectively. For all the lipid species, the side chain was identified thanks to MS/MS data in negative ion mode.

Statistical analysis

A false discovery rate (FDR-adjusted $p < 0.01$) controlling procedure was performed to assess the statistical significance of the concentration differences of the identified lipids from cell extracts of BAK-treated cells vs control cells as previously

described [22]. Each experiment was performed independently at least five times. ANOVA, Dunnett’s test, and Student’s t -test were performed using GraphPad Prism 8 software (GraphPad Software, La Jolla, CA) with a risk set at 0.05 (* $p < 0.05$, ** $p < 0.01$, *** $p < 0.001$).

Results and discussion

Validation and technical adaptation of the CM reaction

We firstly demonstrated that a pure commercial phosphatidylcholine lipid readily reacts with (*Z*)-but-2-ene-1,4-diyl diacetate used as CM partner. The reaction was performed under mild conditions in the presence of the Grubbs catalyst of second generation. It is noteworthy that the symmetrical alkene used is highly reactive and prevents the formation of ethylene and ethylene CM adducts that would render analysis more complex. A first assay was performed at the micromole scale. Briefly, 6.3 μ mol (5.0 mg) of PC (18:0/18:1 $\Delta 9$) diluted in CH_2Cl_2 (0.5 mL) was treated at 40 °C for 2 h with 5 equivalents of (*Z*)-but-2-ene-1,4-diyl diacetate in the presence of 5 mol% of Grubbs’ catalyst. The reaction mixture was subsequently diluted (1/10,000) with MeOH and analyzed through direct infusion on a Synapt G2 (Q-ToF) high-resolution mass spectrometer. The resulting mass spectrum displayed an intense peak at m/z 770.4953 corresponding to the $[\text{M}+\text{Na}]^+$ adduct PC (18:0/AcO-11:1 $\Delta 9$) (ESM Fig. S1). The proximal C10–C18 moiety of the unsaturated FA chain has therefore been replaced by a 2-acetoxyethyl-1-ylidene moiety. In contrast, the distal part, *i.e.*, the methyl end alkene, anticipated to be undec-2-en-1-yl acetate, was not detected.

Given that, in a typical biological sample, the overall content in phospholipids is of about tens of nanomole for 10^6 cells, a scale down was needed. However, the usual concentration used in CM reaction would, if transpose at a nanomole scale, require an amount of CH_2Cl_2 so small that it would immediately evaporate at 40 °C. This led us devising neat reaction conditions using circa one equivalent of catalyst compared to the lipids and 50 equivalents of the CM partner. Using 2 nmol of the previous PC (18:0/18:1 $\Delta 9$), CM was performed as described hereafter. Briefly, Grubbs’ catalyst (0.1 M) was pre-treated with 50 equivalents of (*Z*)-but-2-ene-1,4-diyl diacetate in CH_2Cl_2 at 40 °C for 2 h to afford a Ru carbene bearing the CM partner. This solution was diluted, an appropriate volume was added to 2 nmol of PC (18:0/18:1 $\Delta 9$), and the solvent was subsequently removed under a flow of argon at 40 °C (ESM Fig. S2). The reaction mixture was heated in a sealed tube at 40 °C for 2 h, diluted in 100 μ L of a $\text{CHCl}_3/\text{MeCN}/\text{H}_2\text{O}/i\text{-PrOH}$ (20/30/10/30, v/v) mixture, and 5 μ L was injected

in the LC-MS/MS system, the analysis being performed using previously described conditions [22–24].

In positive ion mode, the extracted ion chromatograms (EIC) at m/z 748.5123 and m/z 788.618 showed a first peak at $t_R = 4.1$ min and a second at $t_R = 7.1$ min corresponding to the $[M+H]^+$ of PC (18:0/AcO-11:1 $\Delta 9$) and native PC (18:0/18:1 $\Delta 9$), respectively (Fig. 1A). The MS/MS spectra displayed an intense peak at m/z 184.07 characteristic of the PC polar head group (Fig. 1B and C). In negative ion mode, the EIC at m/z 732.479 showed an intense peak assigned to the $[M-CH_3]$ PC (18:0/AcO-11:1 $\Delta 9$) confirming information obtained under positive ion conditions. In addition, negative ion mode is required to identify the FA side chains. Indeed, the MS/MS spectrum displayed at m/z 283.26, a peak diagnostic of stearate in sn_1 position, and at m/z 241.1453, a second peak corresponding to 11-acetoxyundec-9-enoate (FA (AcO-11:1 $\Delta 9$)) in sn_2 position (Fig. 1E). These product ions are indicative of an oleate in sn_2 position and therefore allowed to unambiguously locate the double bond.

HCl pretreatment to prevent deleterious effect of amine on Grubbs catalyst

On the one hand, it has long been established that the Grubbs catalysts are poisoned by amines [28]. On the other hand, among the phospholipid subclasses commonly encountered in biological samples, phosphatidylethanolamine (PE) and phosphatidylserine (PS) display basic primary amine functions. Accordingly, when a mixture of 20 commercially available standard phospholipids (ESM Table S1) including PE and PS subclasses is submitted to our CM conditions, it gave a very poor yield of the expected CM products. Indeed, CM afford PC (18:0/AcO-11:1 $\Delta 9$) with approximately 20% yield when it is performed on a pure PC (18:0/18:1 $\Delta 9$) and dramatically decreases to 5% when this PL is included in the standard lipid mixture (Fig. 2B and C). To prevent the deleterious effect of basic amines, the lipid mixture was pre-treated with 1M HCl solution to give innocuous ammonium chlorides [28]. CM performed under these conditions allowed to recover yields closed to those obtained with pure PC (18:0/18:1 $\Delta 9$)

Fig. 1 Analytical features of PC (18:0/18:1 $\Delta 9$) and its CM product PC (18:0/AcO-11:1 $\Delta 9$). **A** EIC at m/z 788.618 and m/z 748.5123 corresponding to $[M+H]^+$ PC (18:0/18:1 $\Delta 9$) and PC (18:0/AcO-11:1 $\Delta 9$). PC (18:0/18:1 $\Delta 9$) and PC (18:0/AcO-11:1 $\Delta 9$) MS/MS spectra in **B**, **C** positive and **D**, **E** negative ion mode

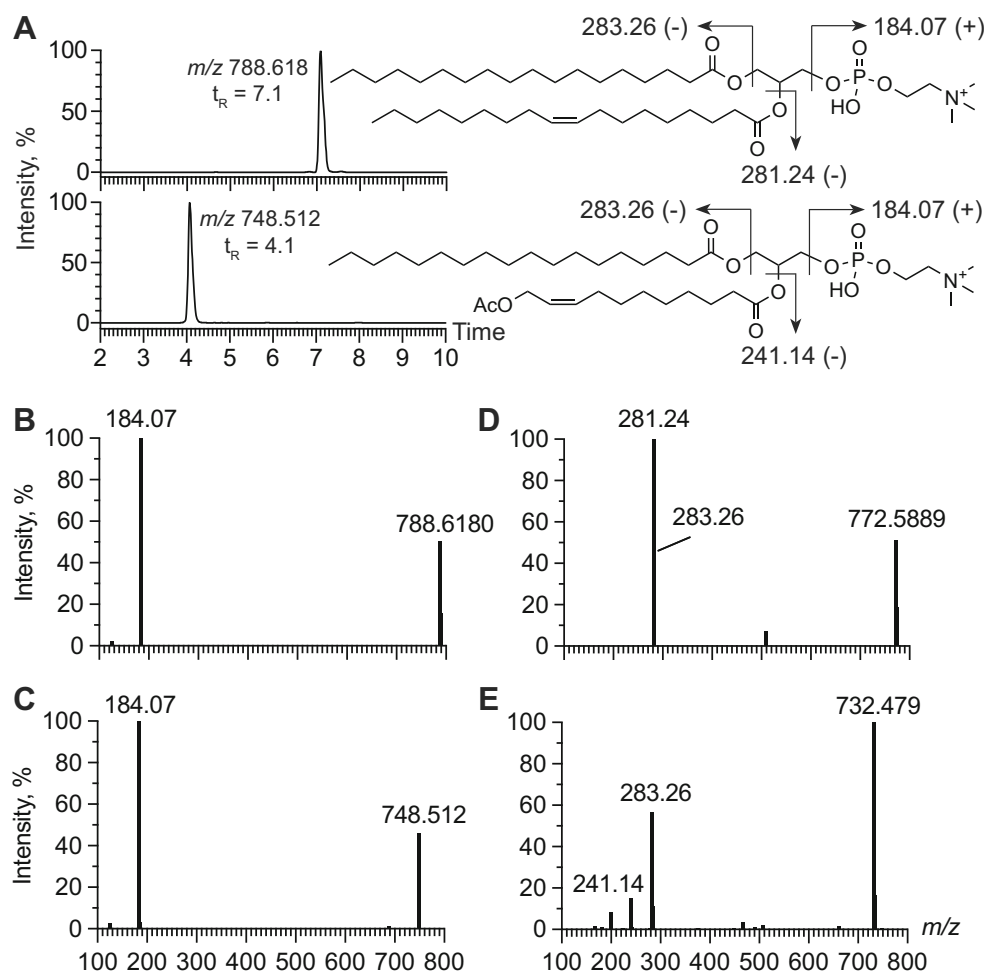
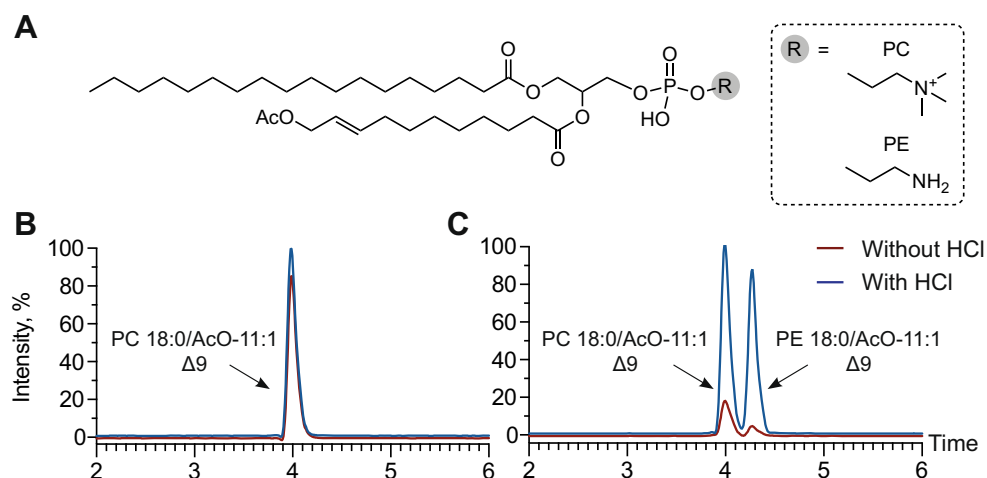


Fig. 2 HCl pretreatment to prevent the inhibition of Grubbs' catalyst by amino groups. **A** CM product structures. **B** EIC at m/z 748.5142 corresponding to the $[M+H]^+$ ion of PC (18:0/AcO-11:1 Δ 9) without and with HCl pretreatment in a reaction medium containing pure PC (18:0/18:1 Δ 9) specie. **C** EIC at m/z 748.5142 and m/z 706.467 corresponding to the $[M+H]^+$ ion of PC (18:0/AcO-11:1 Δ 9) and PE (18:0/AcO-11:1 Δ 9) without and with HCl pretreatment in a reaction medium containing a mixture of PC and PE species



(Fig. 2C). For PE and PS species, HCl pretreatment allow to increase the yield by 25-fold. This yield is indeed about 20% for PC but also for other PL investigated under the aforementioned experimental conditions, *i.e.*, 2 h at 40°C. Thus, HCl pretreatment proves essential for CM reactions performed on lipid of biological lipid mixtures, while being sufficiently mild to avoid degradation of significant amount of lipids in most cases. This degradation was estimated to be less than 10% for the investigated lipid subclasses (data not shown).

Evaluating the versatility of CM reaction using phospholipids containing various FA side chains

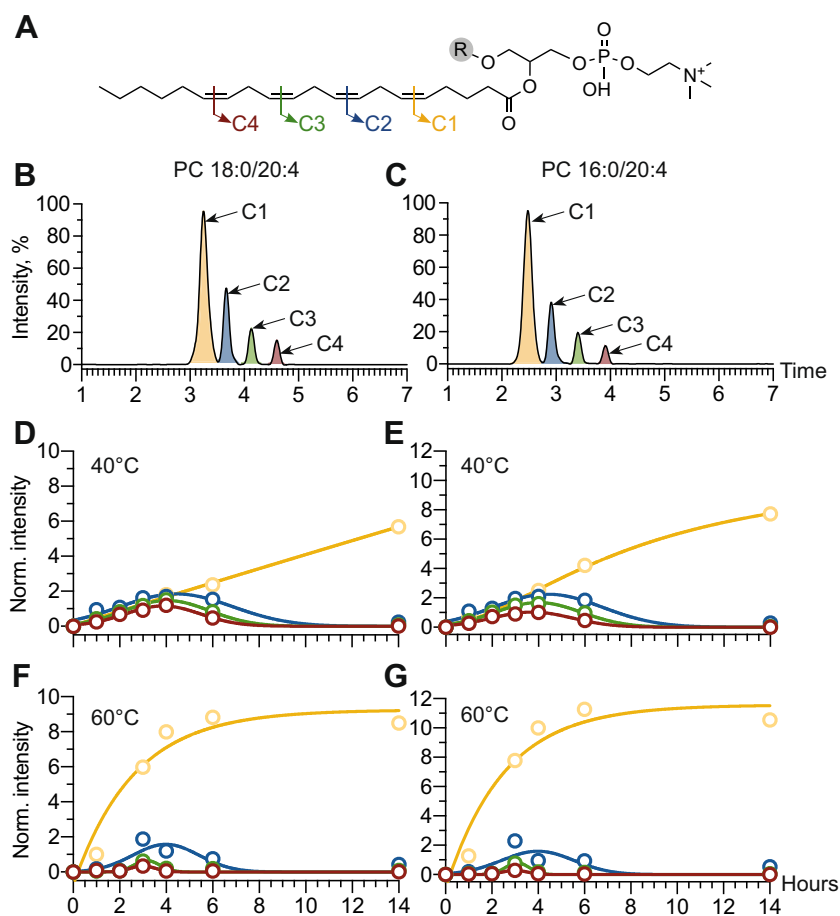
The mixture of commercial lipid standards used contains mono- and polyunsaturated FA side chains representative of FAs commonly encountered in biological samples. While phospholipids such as PC (18:0/18:1 Δ 9) lead to a single CM product, all C=C bonds present in phospholipids containing PUFA chain are also expected to react but leading however to the formation of several CM products. Indeed, when CM was performed on PC (18:0/20:4 Δ 5, Δ 8, Δ 11, Δ 14) under the previous conditions, it led to 4 CM products: PC (18:0/AcO-16:4 Δ 5, Δ 8, Δ 11, Δ 14) (C4), PC (18:0/AcO-13:3 Δ 5, Δ 8, Δ 11) (C3), PC (18:0/AcO-10:2 Δ 5, Δ 8) (C2), and PC (18:0/AcO-7:1 Δ 5) (C1) (Fig. 3A and B; ESM Fig. S3). Detecting simultaneously all possible CM products in the final reaction mixture may be regarded as a gold standard as it allows locating all the double bonds and hence identifying unambiguously phospholipids containing PUFA. To ensure that the final reaction mixture contains all the CM products at concentrations letting optimal detection by mass spectrometry, a kinetic study was carried out by varying the temperatures with PC (18:0/20:4) and PC (16:0/20:4) (Fig. 3D–G). Whatever the reaction time, chromatographic peaks corresponding to C1 and C4 products exhibited the highest and the lowest AUC compared to C2 and C3 (Fig. 3D and E). As expected, during the reaction, C2, C3, and C4 decreased in

favor of C1. Moreover, at 4 h of reaction at 40°C, C2, C3, and C4 displayed suitable AUC and thus represent the best compromise to identify all the C=C bonds' position (Fig. 3D and E). In contrast, CM carried out at 60 °C mainly led to C1 products with a 4 times increased yield compared to 40°C, whatever the PC species (Fig. 3F and G) while C2, C3, and C4 were sparsely detected in that case.

Several phospholipids included in the standard lipid mixture contain two unsaturated FA side chains, and we expected CM to occur at both sn_1 and sn_2 positions randomly (Fig. 4B–D). This means that for instance PC (22:1/22:1 Δ 13/ Δ 13) should give 3 CM products. Using this PC, we observed in positive ion mode that EIC at m/z 898.7252 and m/z 818.5181 displays two peaks at $t_R = 8.1$ min and $t_R = 2.3$ min corresponding to the $[M+H]^+$ ions of respectively native PC (22:1/22:1 Δ 13/ Δ 13), and PC (AcO-15:1/AcO-15:1 Δ 13/ Δ 13) issuing from a double CM process (Fig. 4B). A third peak at m/z 858.6216 and $t_R = 5.7$ min is displayed; it corresponds to both PC (22:1/AcO-15:1 Δ 13/ Δ 13) and its regioisomer PC (AcO-15:1/22:1 Δ 13/ Δ 13) which are almost co-eluted. On MS/MS spectra, an intense peak at m/z 184.07 corresponds to the PC polar head group (ESM Fig. S4). In negative ion mode, MS/MS spectrum exhibited peaks at m/z 337.31 and at m/z 297.21 due to respectively docos-13-enoate and 15-acetoxypentadec-13-enoate. While m/z 337.31 is due to native PC (22:1/22:1 Δ 13/ Δ 13), product ions at m/z 297.21 are associated with CM-modified PC which allows pinpointing the C=C bond (Fig. 4E–G). Ring closure metathesis was also possible in that case, and interestingly, PC (22:1/22:1 Δ 13/ Δ 13) gave a 30-membered ring product detected as a $[M+H]^+$ at m/z 646.45 at $t_R = 3.4$ min (Fig. 4B).

It must be emphasized that we performed the cross-metathesis at 60°C or below during a short period of time, and that in addition no terminal alkene is present in the reaction medium. Therefore, the conditions we used allow avoiding the formation of fragile methyldiene ruthenium that degrades into detrimental hydridoruthenium species

Fig. 3 CM applied on polyunsaturated PC. **A** PC containing arachidonate chain. **B** EIC of CM products of PC (18:0/20:4 $\Delta 5$, $\Delta 8$, $\Delta 11$, $\Delta 14$) at m/z 812.5456, m/z 772.5141, m/z 732.4826, and m/z 692.4511 corresponding to $[M+H]^+$ C4, C3, C2, and C1. **C** EIC of CM products of PC (16:0/20:4) at m/z 784.5142, m/z 744.4827, m/z 704.4512, and m/z 664.4197 corresponding to $[M+H]^+$ ions of C4, C3, C2, and C1. **CM kinetics** on PC (18:0/20:4 $\Delta 5$, $\Delta 8$, $\Delta 11$, $\Delta 14$) and PC (16:0/20:4 $\Delta 5$, $\Delta 8$, $\Delta 11$, $\Delta 14$) at **D**, **E** 40°C and **F**, **G** 60°C



responsible for alkene shift. So, no double bond mislocation due to unsaturation shift was observed in our case [29, 30].

An UHPLC-MS/MS workflow for the analysis of lipids down to double bond location

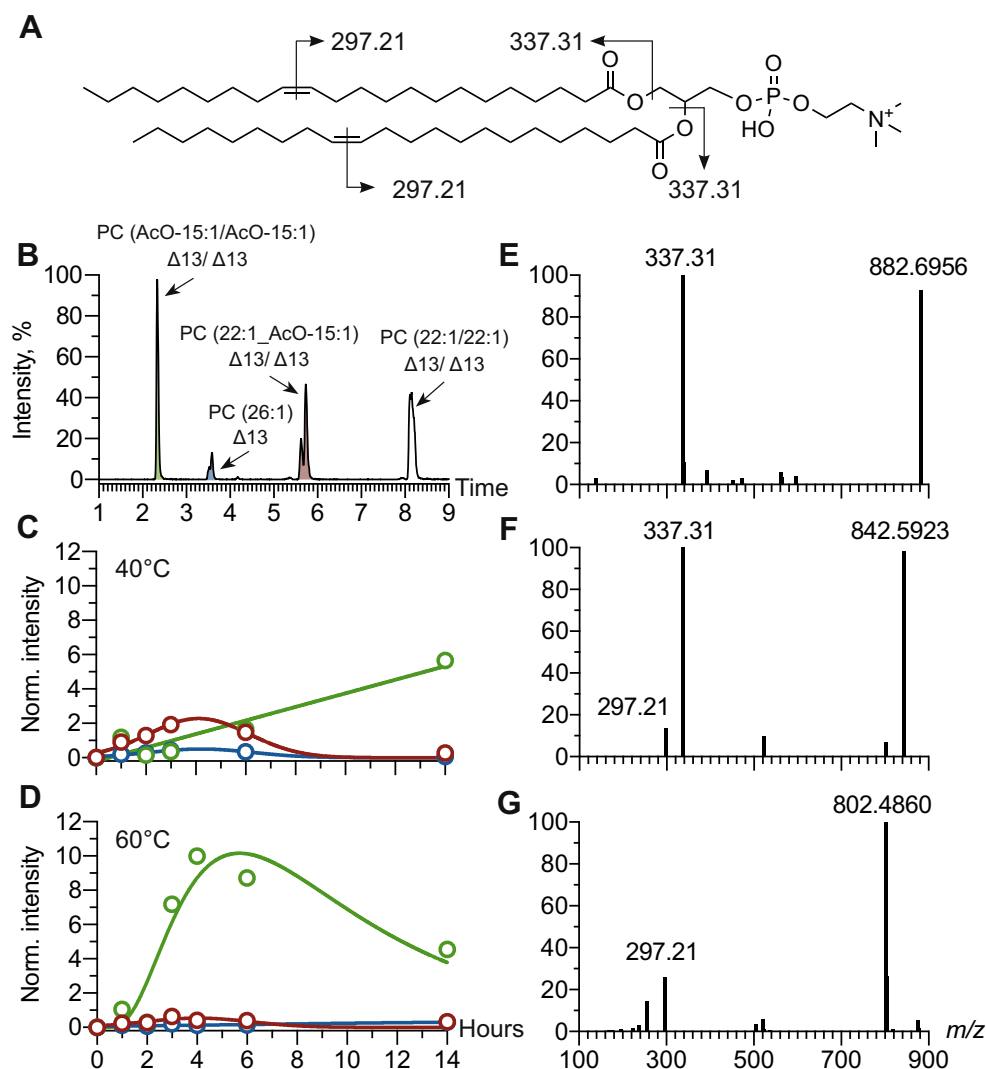
Within PC subclass, CM was successfully applied to identify the double bond location of lipid species commonly encountered in biological samples, *i.e.*, PL containing SFA/MUFA, SFA/PUFA, and MUFA/MUFA side chains. The kinetic profiles we previously described for PC at 40 and 60°C were reproducibly observed for all lipid species whatever the phospholipid subclasses considered, *i.e.*, PE, PS, PG, and PI, as well as for several sphingolipids and glycerolipids including Cer, SM, DG, and TG, respectively (ESM, Table S1 and Figs. S5–S24). CM reaction was thus applied to locate double bond in 10 lipid subclasses belonging to 4 classes. An amount of about 10 pmol per lipid species was used indicating an appropriate sensitivity of the method.

To assess the efficiency of the proposed method, lipid extracts from human epithelial corneal cell line (HCE) were investigated. For this purpose, individual biological sample containing 3 million cells was prepared and analyzed by UHPLC-HRMS/MS. In a first step, based on t_R and MS

data managed as previously described [22], we were able to identify at the subclass level 270 lipid species. For example, to $t_R = 6.47$ min and m/z 760.5870, the lipid species PC (34:1) was associated (Figs. 5A and 6B; ESM Table S2). In a second step dealing with negative ion mode MS/MS data, the fatty acid side chain composition of the major regioisomer was determinate for 98 phospholipids, 41 glycerolipids, and 31 sphingolipids (Fig. 5B; ESM Table S2). This second step allowed to annotate PC (16:0/18:1) as the major regioisomer of PC (34:1) detected in HCE cells. Among the 170 lipid species annotated at the fatty acyl side chain level, 150 were eligible to CM reaction as they contain one double bond at least. Finally, a third step based on CM reaction and LC-ESI-HRMS/MS analysis allows to identify double bond location in 50 phospholipids, 25 glycerolipids, and 30 sphingolipids. It corresponds to approximately the 2/3 of the candidate lipid species (Fig. 5B; ESM Table S2). This last step allowed to identify PC (16:0/18:1) as PC (16:0/18:1 $\Delta 9$).

It is noteworthy that the proposed method inevitably requires two distinct steps, the first based on the analysis of LC-MS/MS data of native lipid species gives access to the subclass and to the nature and position of the fatty acid chains and the second, based on the analysis of CM products by LC-

Fig. 4 CM on phospholipids containing unsaturated FA chains both on sn_1 and sn_2 positions. **A** Structure of PC (22:1/22:1 13Z/13Z) and m/z value of product ions corresponding to FA chains of CM products in ESI⁺ mode. **B** EIC at m/z 818.5180 (t_R = 2.3 min), m/z 646.4444 (t_R = 3.5 min), m/z 858.6216 (t_R = 5.7 min), and m/z 898.72 (t_R = 8.2 min) corresponding to PC (AcO-15:1/AcO-15:1 Δ 13/ Δ 13), PC (26:1 13E), PC (22:1/AcO-15:1 Δ 13/ Δ 13), and native PC (22:1/22:1 Δ 13/ Δ 13) respectively. Kinetic study of CM products of PC 22:1/22:1 Δ 13/ Δ 13 at **C** 40°C and **D** 60°C. Negative ion mode MS/MS spectra of **E** PC (22:1/22:1 Δ 13/ Δ 13), **F** PC (22:1/AcO-15:1 Δ 13/ Δ 13), and **G** PC (AcO-15:1/AcO-15:1 Δ 13/ Δ 13)



MS/MS, allows to locate the position of the double bond. Moreover, as the distal part of the native lipid being lost following CM reaction, a definitive double bond location may be difficult in some cases. For example, PE (16:0/18:1) and PE (16:0/16:1) were both identified in HCE cells. Following CM reaction and LC-HRMS/MS analysis, a peak at t_R = 3.55 min and m/z 676.4187 corresponding to the $[M-H]^-$ ion of PE (16:0/AcO-11:1 Δ 9) was detected. Anyone can conclude that PE (16:0/18:1) and PE (16:0/16:1) are Δ 9 regioisomers. However, another peak at t_R = 4.12 min and m/z 704.45 was also observed; it corresponds to the $[M-H]^-$ ion of PE (16:0/AcO-13:1 Δ 11), the CM product of PE (16:0/18:1 Δ 11). This second peak being 10-fold lower than the first one suggests that PE (16:0/18:1 Δ 9) and PE (16:0/16:1 Δ 9) are the major isomer species. However, the detection of PE (16:0/AcO-13:1 Δ 11) also indicates that PE (16:0/18:1) is a mix of Δ 9 and Δ 11 isomers. Another limitation of the proposed method is

related to sample preparation. Indeed, the HCl pretreatment leads to plasmalogen hydrolysis preventing double bond location in these alkenyl phospholipids. Finally, a last weakness deals with sensitivity. Indeed, for lipids in low abundance or poorly ionizable in ESI, double bond location may be impossible due to lack of MS/MS data and/or CM product in a sufficient amount to be detected. This drawback may be circumvented using larger biological samples or using CM partners that could transfer an ionizable functional group.

Structural lipidomics, an entry to investigate the toxic effect of benzalkonium chloride

In human corneal epithelial cell line, we previously reported that benzalkonium chloride (BAK), a quaternary ammonium, has a major impact on the lipidome; however, at that time, we were not able to determine lipid double bond location [25, 31].

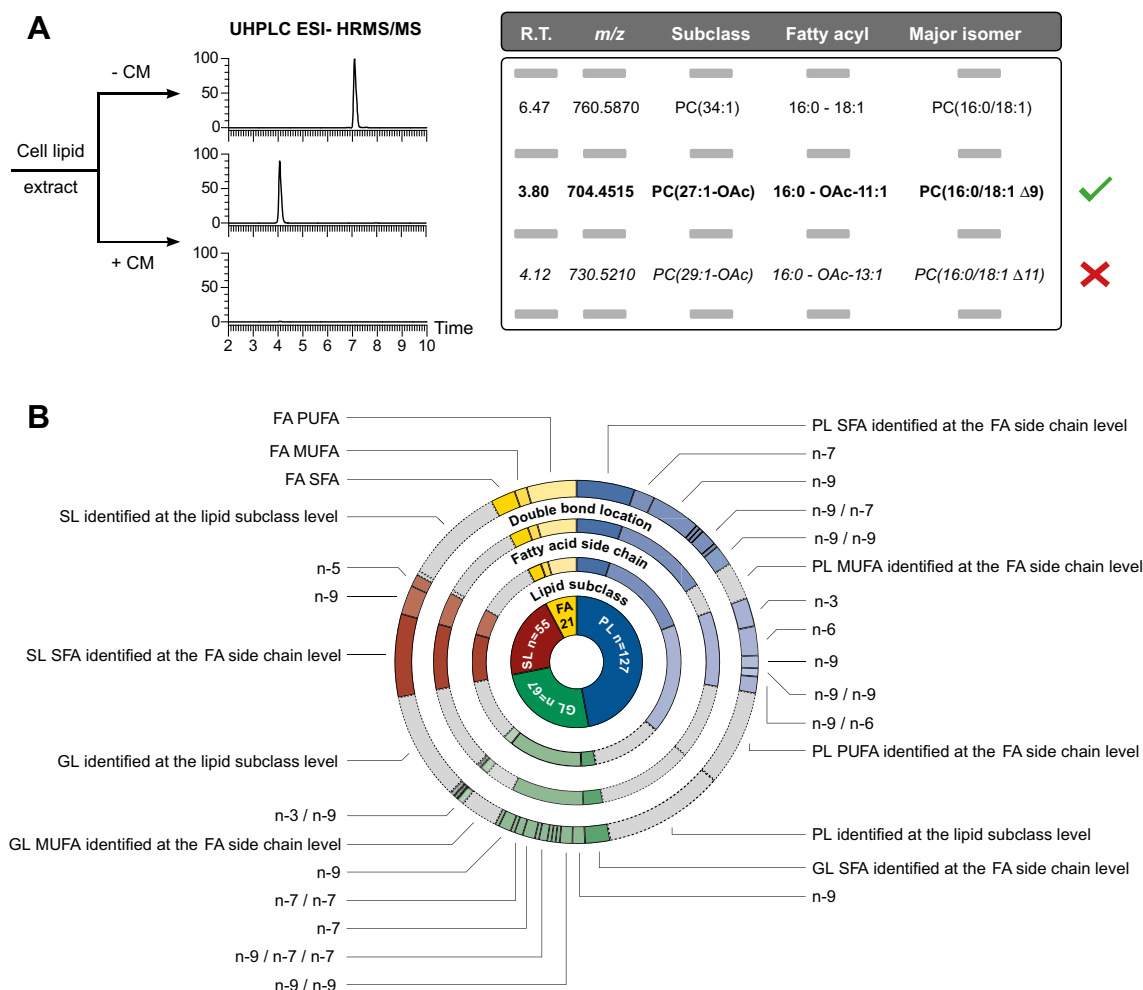


Fig. 5 Determination of the double bond location in lipid species within human corneal cells. **A** Workflow to pinpoint double bonds in lipid species in biological samples. **B** Lipid identification of human corneal

cells (3 million cells/sample) from inside to outside the pie chart: lipid subclass, fatty acid side chain, and double bond location levels

We thus applied the proposed method to this biological sample to go deeper into the lipid homeostasis disruption induced by BAK on corneal cells. BAK is the main preservative in multidose eye drops, which have long-term indication for glaucoma and dry eye disease (DED), two diseases deeply

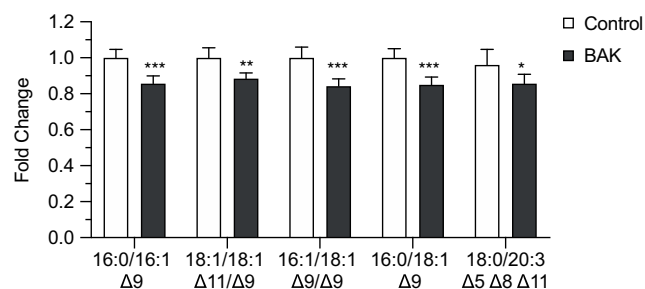
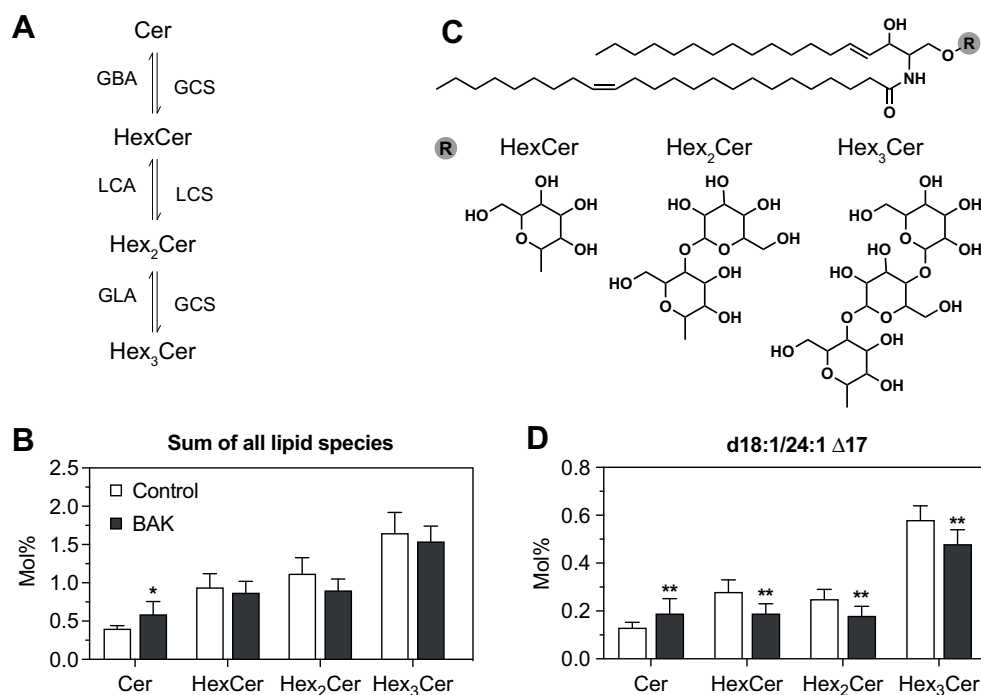


Fig. 6 Effect of BAK on the cell content of PC species containing Δ 9 FA. Results are expressed as mean fold change \pm standard deviation compared to control (multiple t-test with FDR rate at 0.01. $n = 5$. * $p < 0.05$; ** $p < 0.01$; *** $p < 0.001$)

impacting quality of life [32–35]. Because of its pro-inflammatory and pro-apoptotic effects, BAK may be responsible for DED or worsen it. HCE cells exposed to BAK is thus a well-established toxicological model of corneal damage [32, 35, 36], thanks to which we have previously demonstrated a striking decrease in PC species whatever the FA side chains considered [31]. Using the developed method, we succeeded at determining the structure of the five following PC species displaying an homeostasis change following BAK exposure. Indeed, in PC (18:1/18:1), FA side chains were identified as an oleyl (18:1 Δ 9) and an octadec-11-enoyl (18:1 Δ 11) (ESM Fig. S25). In PC (16:1/18:1), FA chains were identified as palmitoleyl (16:1 Δ 9) and oleyl (18:1 Δ 9) in sn_1 and sn_2 , respectively. PC (16:0/18:1) and PC (16:0/16:1) contain oleyl (18:1 Δ 9) and palmitoleyl (16:1 Δ 9) in sn_2 position respectively (ESM Fig. S26–S27). Finally, PC (18:0/20:3) contained an eicosatrienoyl (20:3 Δ 5 Δ 8 Δ 11) in sn_2 position. Therefore, regarding PC subclass, our method has revealed BAK-induced changes especially on lipid species containing

Fig. 7 Effect of BAK on sphingolipid metabolism. **A** Biosynthesis pathway of sphingolipid metabolism. **B** Effect of BAK on the total cell content of Cer, HexCer, Hex₂Cer, and Hex₃Cer. **C** Structure of Cer, HexCer, Hex₂Cer, and Hex₃Cer containing d18:1/24:1 Δ 17 side chain. **D** Effect of BAK on the total cell content of Cer, HexCer, Hex₂Cer, and Hex₃Cer containing d18:1/24:1 Δ 17 side chain



double bond located at the Δ 9 position (Fig. 6). In cell, biosynthesis of Δ 9 MUFA using SFA species as substrate involves stearoyl CoA desaturase (SCD). The decrease in PC levels may thus be related to a change in the gene expression of SCD enzyme. Consistent with this, it has been previously described that BAK exposure leads to an increase in the gene expression of SCD enzyme [37]. To fully demonstrate that BAK induces ocular damage by targeting Δ 9 FA metabolism through SCD enzyme, the investigation of enzymes involved in FA elongation and desaturation metabolism remains to be carried out.

Regarding sphingolipids, an increase in several ceramide species was exhibited following BAK exposure (Fig. 7C). Nevertheless, no global change in the cell content of MonohexosylCeramide (HexCer), DihexosylCeramide (Hex₂Cer), and TrihexosylCeramide (Hex₃Cer) was displayed (Fig. 7B). HexosylCeramides derive from ceramide through the addition of one, two, or three hexoses (Fig. 7A). Thanks to CM and LC-HRMS/MS, we identify that whatever the sphingolipid subclass considered, the FA (24:1) is the Δ 17 regioisomer (Fig. 7B). In HCE cells exposed to BAK, ceramide containing FA (24:1 Δ 17) increased while the corresponding HexCer, Hex₂Cer, and Hex₃Cer decreased (Fig. 7D; ESM Tables S2 and S3). This result may suggest that BAK induce specific hexosylceramide hydrolase to produce these pro-apoptotic lipid species. Interestingly, biosynthesis of FA (24:1 Δ 17) involves the elongation of FA (18:1 Δ 9) which originate from stearic acid through the action of SCD enzyme. The

developed methods thus prove to be valuable to understand the impact of BAK on lipid species whatever the class considered. Therefore, SCD appears to be a key enzyme in the sphingolipid and phospholipids homeostasis disruption induced by BAK in HCE cells.

Conclusion

In summary, we have demonstrated that associating Grubbs catalyzed CM reaction and LC-MS/MS analysis allows an accurate identification of a broad scope of lipid isomers through a quite simple and highly reproducible procedure. We have optimized conditions to obtain all the possible CM products enabling a full identification of MUFA and PUFA with a sensitivity allowing the analysis of biological samples. We are currently pursuing this study testing CM partners that could transfer an ionizable functional group allowing the identification of the distal moiety of FA chains. Furthermore, no sophisticated adaptation of the LC-MS system previously developed is needed to analyze complex lipid samples with our method. CM products exhibit same fragmentation patterns in MS/MS as native lipids which thus facilitate the identification. Nevertheless, in some cases, a definitive double bond location may be difficult, the distal part of the native lipid being lost following CM reaction. Furthermore, a key challenge remains regarding the post-acquisition of the large amount of data in the case of complex lipid extracts, especially for the reliable attribution of CM products to native lipid species.

Regarding this specific point, a data processing strategy is currently in progress and will be the subject of a dedicated study.

Supplementary Information The online version contains supplementary material available at <https://doi.org/10.1007/s00216-021-03438-w>.

Acknowledgements The authors thank the Centre Hospitalier National d'Ophthalmologie des Quinze-Vingts, Région Ile-de-France.

Author contribution Conceptualization: R. Magny, A. Regazzetti, F. Brignole-Baudouin, N. Auzeil, E. Roulland. Methodology: R. Magny, A. Regazzetti, K. Kessal, F. Brignole-Baudouin, N. Auzeil, E. Roulland. Formal analysis: R. Magny, A. Regazzetti, K. Kessal, F. Brignole-Baudouin, N. Auzeil, E. Roulland. Supervision: C. Baudouin, S. Mélik-Parsadaniantz, O. Laprévote. Validation: F. Brignole-Baudouin, N. Auzeil, E. Roulland. Writing—original draft: R. Magny, A. Regazzetti, K. Kessal, F. Brignole-Baudouin, N. Auzeil, E. Roulland. Writing—review and editing: C. Baudouin, S. Mélik-Parsadaniantz, O. Laprévote, F. Brignole-Baudouin, N. Auzeil, E. Roulland.

Funding This study was funded by Sorbonne Université, Université de Paris, the Institut National de la Santé et de la Recherche Médicale and the Centre National de la Recherche Scientifique (CNRS). This work was completed with the support of the Programme Investissements d'Avenir IHU FOReSIGHT (ANR-18-IAHU-01).

Declarations

Conflict of interest The authors declare no competing interests.

References

- Wenk MR. Lipidomics: new tools and applications. *Cell*. 2010;143:888–95.
- Meikle PJ, Summers SA. Sphingolipids and phospholipids in insulin resistance and related metabolic disorders. *Nat Rev Endocrinol*. 2017;13(2):79–91.
- Fahy E, Subramaniam S, Brown HA, Glass CK, Merrill AH, Murphy RC, et al. A comprehensive classification system for lipids. *J Lipid Res*. 2005 [cited 2019 Aug 23];46(5):839–62.
- Fahy E, Subramaniam S, Murphy RC, Nishijima M, Raetz CRH, Shimizu T, et al. Update of the LIPID MAPS comprehensive classification system for lipids. *J Lipid Res*. 2009;50(Supplement):S9–14.
- Serhan CN, Savill J. Resolution of inflammation: the beginning programs the end. *Nature Immunology*. 2005;6:1191–7.
- Martinez-Seara H, Róg T, Pasenkiewicz-Gierula M, Vattulainen I, Karttunen M, Reigada R. Interplay of unsaturated phospholipids and cholesterol in membranes: effect of the double-bond position. *Biophys J*. 2008;95(7):3295–305.
- Gordon WC, Bazan NG. Mediator lipidomics in ophthalmology: targets for modulation in inflammation, neuroprotection and nerve regeneration. *Curr Eye Res*. 2013;38(10):995–1005.
- Pham TL, Bazan HEP. Docosanoid signaling modulates corneal nerve regeneration: effect on tear secretion, wound healing, and neuropathic pain. *J Lipid Res*. 2020 Aug 11 [cited 2020 Dec 10];jlr.TR120000954.
- Zhang W, Zhang D, Chen Q, Wu J, Ouyang Z, Xia Y. Online photochemical derivatization enables comprehensive mass spectrometric analysis of unsaturated phospholipid isomers. *Nat Commun*. 2019;10(1):1–9. Available from: <https://doi.org/10.1038/s41467-018-07963-8>.
- Züllig T, Trötzmüller M, Köfeler HC. Lipidomics from sample preparation to data analysis: a primer. *Anal Bioanal Chem*. 2019: 2191–209.
- Wang J, Wang C, Han X. Tutorial on lipidomics. *Analytica Chimica Acta*. Elsevier B.V. 2019;1061:28–41.
- Holčapek M, Liebisch G, Ekroos K. Lipidomic analysis. *Anal Chem*. 2018 [cited 2019 Oct 15];90(7):4249–57.
- Porta Siegel T, Ekroos K, Ellis SR. Reshaping lipid biochemistry by pushing barriers in structural lipidomics. *Angew Chemie*. 2019;131(20):6560–9.
- Klein DR, Brodbelt JS. Structural characterization of phosphatidylcholines using 193 nm ultraviolet photodissociation mass spectrometry. *Anal Chem*. 2017 [cited 2020 Dec 10];89(3):1516–22.
- Poad BLJ, Pham HT, Thomas MC, Nealon JR, Campbell JL, Mitchell TW, et al. Ozone-induced dissociation on a modified tandem linear ion-trap: observations of different reactivity for isomeric lipids. *J Am Soc Mass Spectrom*. 2010;21(12):1989–99.
- Ma X, Xia Y. Pinpointing double bonds in lipids by paterno-büchi reactions and mass spectrometry. *Angew Chemie - Int Ed*. 2014;53(10):2592–6. [cited 2020 Dec 10] Available from: <https://doi.org/10.1002/anie.201310699>.
- Zhao X, Zhang W, Zhang D, Liu X, Cao W, Chen Q, et al. A lipidomic workflow capable of resolving: Sn - And CC location isomers of phosphatidylcholines. *Chem Sci*. 2019 [cited 2021 Mar 22];10(46):10740–8.
- Kuo TH, Chung HH, Chang HY, Lin CW, Wang MY, Shen TL, et al. Deep lipidomics and molecular imaging of unsaturated lipid isomers: a universal strategy initiated by mCPBA epoxidation. *Anal Chem*. 2019 [cited 2020 Dec 10];91(18):11905–15.
- Chatterjee AK, Choi TL, Sanders DP, Grubbs RH. A general model for selectivity in olefin cross metathesis. *J Am Chem Soc*. 2003 [cited 2020 Dec 10];125(37):11360–70.
- Kwon Y, Lee S, Oh D-C, Kim S. Simple determination of double-bond positions in long-chain olefins by cross-metathesis. *Angew Chemie*. 2011;123(36):8425–8.
- Araki-Sasaki K, Ohashi Y, Sasabe T, Hayashi K, Watanabe H, Tano Y, et al. An SV40-immortalized human corneal epithelial cell line and its characterization. *Invest Ophthalmol Vis Sci*. 1995;36(3):614–21.
- Magny R, Regazzetti A, Kessal K, Genta-Jouve G, Baudouin C, Mélik-Parsadaniantz S, et al. Lipid annotation by combination of UHPLC-HRMS (MS), molecular networking, and retention time prediction: application to a lipidomic study of in vitro models of dry eye disease. *Metab*. 2020;10(6):225.
- Lanzini J, Dargère D, Regazzetti A, Tebani A, Laprévote O, Auzeil N. Changing in lipid profile induced by the mutation of Foxn1 gene: a lipidomic analysis of Nude mice skin. *Biochimie*. 2015;118:234–43.
- Petit J, Wakx A, Gil S, Fournier T, Auzeil N, Rat P, et al. Lipidome-wide disturbances of human placental JEG-3 cells by the presence of MEHP. *Biochimie [Internet]*. 2018;149:1–8.
- Magny R, Kessal K, Regazzetti A, Yedder A Ben, Baudouin C, Parsadaniantz SM, et al. Lipidomic analysis of epithelial corneal cells following hyperosmolarity and benzalkonium chloride exposure: new insights in dry eye disease. *Biochim Biophys Acta - Mol Cell Biol Lipids*. 2020 May 11 [cited 2020 May 11];158728.
- Myers OD, Sumner SJ, Li S, Barnes S, Du X. One step forward for reducing false positive and false negative compound identifications from mass spectrometry metabolomics data: new algorithms for constructing extracted ion chromatograms and detecting

- chromatographic peaks. *Anal Chem* [Internet]. 2017 Sep 5 [cited 2020 Feb 18];89(17):8696–703.
27. Hsu FF, Turk J. Electrospray ionization with low-energy collisionally activated dissociation tandem mass spectrometry of glycerophospholipids: mechanisms of fragmentation and structural characterization. Vol. 877, *J Chromatogr B: Analytical Technologies in the Biomedical and Life Sciences*. Elsevier; 2009. p. 2673–95.
 28. Woodward CP, Spiccia ND, Jackson WR, Robinson AJ. A simple amine protection strategy for olefin metathesis reactions. *Chem Commun* [Internet]. 2011 Dec 14 [cited 2020 Dec 10];47(2):779–81.
 29. Hong SH, Day MW, Grubbs RH. Decomposition of a key intermediate in ruthenium-catalyzed olefin metathesis reactions. *J Am Chem Soc* [Internet]. 2004 Jun 23 [cited 2021 May 19];126(24):7414–5.
 30. Soon HH, Wenzel AG, Salguero TT, Day MW, Grubbs RH. Decomposition of ruthenium olefin metathesis catalysts. *J Am Chem Soc* [Internet]. 2007 Jun 27 [cited 2021 May 19];129(25):7961–8.
 31. Magny R, Auzeil N, Olivier E, Kessal K, Regazzetti A, Dutot M, et al. Lipidomic analysis of human corneal epithelial cells exposed to ocular irritants highlights the role of phospholipid and sphingolipid metabolisms in detergent toxicity mechanisms. *Biochimie*. 2020;178:148–57.
 32. Baudouin C, Labbé A, Liang H, Pauly A, Brignole-Baudouin F. Preservatives in eyedrops: the good, the bad and the ugly. *Prog Retin Eye Res* [Internet]. 2010 Jul [cited 2019 Sep 9];29(4):312–34.
 33. Baudouin C, Messmer EM, Aragona P, Geerling G, Akova YA, Benítez-Del-Castillo J, et al. Revisiting the vicious circle of dry eye disease: a focus on the pathophysiology of meibomian gland dysfunction. Vol. 100, *British Journal of Ophthalmology*. BMJ Publishing Group; 2016. p. 300–6.
 34. Baudouin C, Aragona P, Messmer EM, Tomlinson A, Calonge M, Boboridis KG, et al. Role of hyperosmolarity in the pathogenesis and management of dry eye disease: proceedings of the ocean group meeting. *Ocul Surf*. 2013;11(4):246–58.
 35. Brignole-Baudouin F, Desbenoit N, Hamm G, Liang H, Both JP, Brunelle A, et al. A New safety concern for glaucoma treatment demonstrated by mass spectrometry imaging of benzalkonium chloride distribution in the eye, an experimental study in rabbits. *PLoS One*. 2012;7(11).
 36. De Saint JM, Debbasch C, Brignole F, Rat P, Warnet JM, Baudouin C. Toxicity of preserved and unpreserved antiglaucoma topical drugs in an in vitro model of conjunctival cells. *Curr Eye Res*. 2000;20(2):85–94.
 37. Lee M, Joo KM, Choi S, Lee SH, Kim SY, Chun YJ, et al. Nervonoylceramide (C24:1Cer), a lipid biomarker for ocular irritants released from the 3D reconstructed human cornea-like epithelium, MCTT HCETM. *Toxicol Vitro*. 2018;47(September 2017):94–102.

Publisher's note Springer Nature remains neutral with regard to jurisdictional claims in published maps and institutional affiliations.